ATLANTIS PRESS
Advances in Engineering Research (AER), volume 131
3rd Annual International Conference on Electronics, Electrical Engineering and Information Science (EEEIS 2017)

Analysis of Aerodynamic Performance of Tesla Model S by CFD

Qi-Liang WANG[1], Zheng WU[2], Xian-Liang ZHU[3], Li-Li LIU[3], Ying-Chao ZHANG[1,a,*]

[1]State Key Laboratory of Automotive Simulation and Control, Jilin University, Changchun 130022, China

[2]Data Service Division, CH-AUTO Technology Co. Ltd, Beijing, 101300, China

[3]FAW-Volkswagen Automotive Co., Ltd., Changchun 130011, China

[a]yingchao@jlu.edu.cn

[*]Corresponding author

Keywords: Tesla Model S, Aerodynamic performance, Wheel rotation, Ground-clearance, Tread pattern, Drag coefficient.

Abstract. Air drag can affect the cruising ability of pure electric vehicles, especially in the case of high-speed driving. In this project, using 3D laser scanner, we can acquire the point cloud data of the Model S vehicle of Tesla, and the STAR-CCM+ software of Siemens is used to analyse the aerodynamic performance[1] aiming at different working conditions for ground-clearance, tire rotation, tread pattern and so on. The drag coefficient and local flow field data of the vehicle in different working conditions are simulated and the mechanism of flow is analyzed. That could provide experiences for the design of aerodynamic shape of passenger cars. There is practical significance for reference.

Introduction

This paper comes from the cooperation of Jilin University and CH-AUTO Technology Co. Ltd. The cooperation hopes to provide reference for the development of automobile aerodynamics by analyzing the aerodynamic performance of advanced automobile profiles. For this purpose, we have jointly conducted a three-dimensional scan of the Model S vehicle of Tesla[2]. However, due to the complexity of the components in the cabin, there are no modeling and simulation of engine compartment. Tesla models have a public wind tunnel test reported that the coefficient of air drag also has a corresponding value. The simulation conducted in this paper is based entirely on the setup of STAR-CCM+[3] best practices.

Simulation Settings

Car and Wind Tunnel

The simulation takes a lot of effort to catch more details of Tesla Model S by 3D scanning, such as rearview mirror, air grille, tread pattern, windscreen wiper, choke board, door stitch and other details to retain integrity and consistency of the shape with real car.

Copyright © 2017, the Authors. Published by Atlantis Press.
This is an open access article under the CC BY-NC license (http://creativecommons.org/licenses/by-nc/4.0/).

Fig.1. Real car

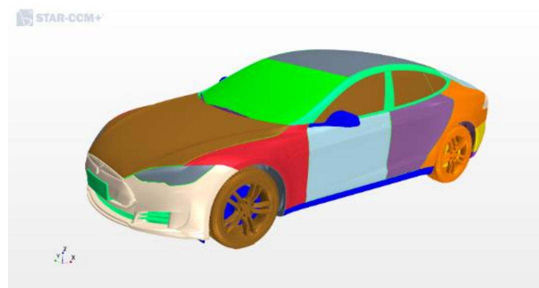

Fig. 2. Digital model

The simulation is based on a virtual wind tunnel, the size is long * wide * high = 55m * 22m * 9m. The boundary condition of the ground is set to slip wall, with the side and top surface are symmetry plane. And the velocity of the air is set to 33.33m/s, with the pressure of outlet is relatively 0pa. For the convenience of calculation, the tire is cut off 5mm from the bottom, as contacted with ground. Ground line and coordinate system rotates a certain angle corresponding to the 3D scan when the vehicle attitude need to be changed, and the ground-clearance is set as table1 in different conditions.

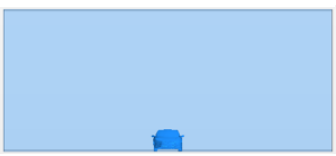

Fig. 3. Front veiw of domain

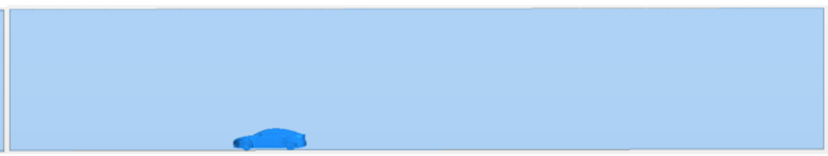

Fig. 4. Side veiw of domain

Physics and Mesh Method

As the complexity of the geometric model details, the simulation is based on K-Epsilon turbulence model with better mesh compatibility [4] for aerodynamic simulation.

The mesh size of the body surface is set to 0.004m-0.01m, and 0.064m, 0.128m, 0.256m three layers of refining domain are set up in the whole wind tunnel. In addition, there are 0.016m and 0.032m two layers of refining domain in the wake area, at the bottom, near the front of the car, the wiper, the rearview mirror and in other areas with large velocity gradient. The total number of vlume mesh cells is 28 million. The simulation uses a 120-core server, after 5000 step steady state calculation, it takes a total of 3h 25min.

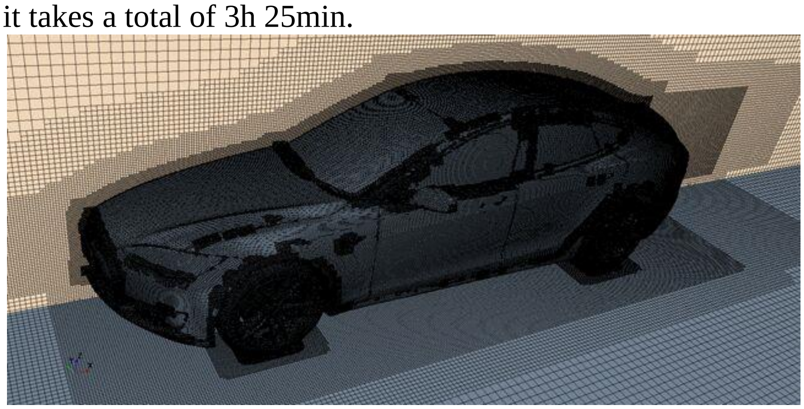

Fig. 5. Volume mesh near the car

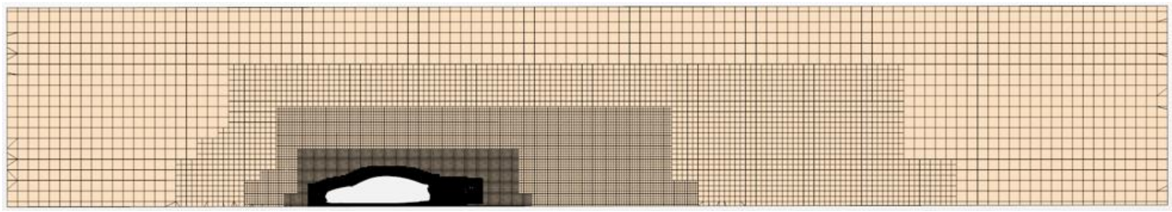

Fig.6. Volume mesh of the whole wind tunnel

Results and Discussion

Overall Coefficient of Drag in Different Conditions

About suspension, Model S has two configurations, spring suspension and air suspension, making its ground clearance also has a corresponding change. At the same time, about the body posture, the half-load conditions are more in line with the actual application of most of the car, so we use half-load and spring suspension as a basic condition.

As shown in Table 1, the simulation results show that the coefficient of aerodynamic force of the vehicle differs in different conditions, including half load condition which indicates air suspension has been adjusted to smallest ground-clearance, and others present spring suspension in different load and tire conditions. It can be seen that when the car is traveling at high speed, the ground clearance is actively adjusted to relatively small, so that air flow at the bottom of the body is accelerated, and the pressure decreases, reducing the aerodynamic lift.

At the same time, the high-speed airflow impact the tail vortex, so that the tail negative pressure area reduced, the air drag is reduced. In addition, through the contrast of bald tires and treads conditions, the impact of the tread pattern on the air drag is relatively large which can not be ignored in the aerodynamic simulation.

Table 1. Overall coefficient of drag in different conditions

Load and conditions	cd	cl	A(m^2)	cd*A
Half load (Ground-clearance144mm,Pattern,Rotation)	0.233	0.041	2.405	0.560365
Half load 1(Ground-clearance 119mm,Pattern,Rotation)	0.232	0.039	2.393	0.555176
No load (Ground-clearance 157mm,Pattern,Rotation)	0.235	0.039	2.418	0.56823
Half load 2(Ground-clearance 144mm,Pattern,Fixed)	0.242	0.073	2.405	0.58201
Half load 3(Ground-clearance 144mm,Slicks,Fixed)	0.231	0.058	2.404	0.555324

Contribution of Different Parts to The Overall Drag

The simulation results show that the contribution of different parts of the outer surface to the coefficient of drag[5] of the vehicle. As can be seen from Table 2, the greatest contribution to air drag is from the face parts in the front of the vehicle. It is due to that the main part of the air drag of car is pressure drag. And the front face is in the windward position with high positive pressure, the contribution of air drag is relatively high.

In the design of the door, the use of hidden handle and built-in window frame, makes the air drag of the door greatly reduced. The choke plate[6] fitted in the front of the vehicle makes the front wheel do less contribution to the air drag than the rear wheel. In addition, the wiper is hidden behind the trailing edge of the front trunk lid, reducing the vortex at the bottom of the front windshield.

Table 2. Drag coefficient of different parts in Half load condition

Parts	Pressure	Shear	Value
FRONT BUMP	0.0638	0.0012	0.0650
FRONT DOOR	-0.0010	0.0019	0.0009
FRONT FENDER	-0.0030	0.0011	-0.0019
FRONT FLOOR	0.0105	0.0071	0.0176
FRONT LAMP	-0.0075	0.0003	-0.0073
FRONT SUSPENSION	0.0018	0.0001	0.0019
FRONT LUGGAGE HOOD	-0.0499	0.0021	-0.0478
FRONT WHEEL HOUSE	0.0103	-0.0002	0.0102
FRONT WHEELS	0.0150	0.0004	0.0154
FRONT WIND SHEILD	-0.0131	0.0018	-0.0113
GAP	0.0021	0.0001	0.0022
GRILLES	0.0359	0.0000	0.0359
LICENSE PLATE	0.0253	0.0000	0.0253
REAR BUMP	0.0212	0.0001	0.0213
REAR DOOR	-0.0014	0.0016	0.0002
REAR FENDER	0.0165	0.0014	0.0179
REAR FLOOR	0.0153	0.0012	0.0165
REAR LAMP	0.0053	0.0001	0.0054
REAR SUSPENSION	0.0056	0.0001	0.0058
REAR LUGGAGE HOOD	0.0139	0.0004	0.0143
REAR WHEEL HOUSE	0.0026	0.0001	0.0028
REAR WHEELS	0.0209	0.0007	0.0215
REAR WINDOW	0.0165	0.0007	0.0172
REARVEIW MIRROR	0.0051	0.0006	0.0057
ROOF	-0.0060	0.0029	-0.0031
SIDE WINDOW	0.0024	0.0015	0.0039
VERTEX GENNERATOR	0.0009	0.0003	0.0011
WINDOW FRAME	-0.0054	0.0012	-0.0042
WIPER	0.0002	0.0000	0.0002
Total	0.2037	0.0289	0.2327

The Effect of Rotation to The Overall Drag

As shown in Fig. 7, the red curve shows the development of the coefficient of drag of the vehicle in the rotation condition of the tire using the tangential velocity [7] settings, and the green line indicates the tire fixing condition. Before the middle of the body, the development trend of the coefficient of drag of the two cases is the same, they also have the same size. However in the rear of the car, the air flow in the bottom of car is accelerated backward due to tire rotation, the impact to the wake reduces the negative pressure [8] behind the tail, leading to 9 counts decline of coefficient of drag.

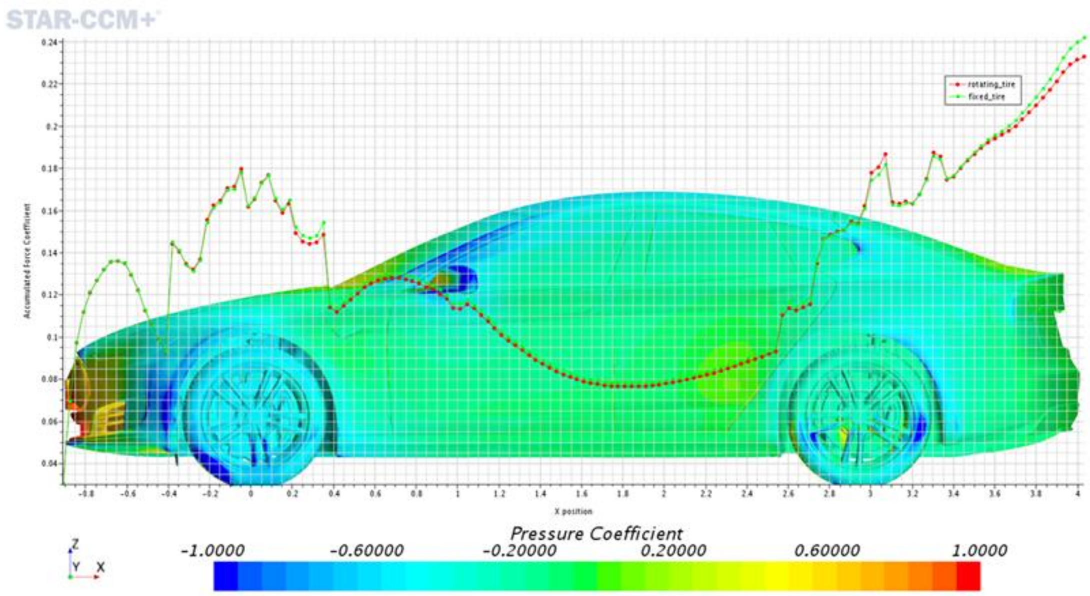

Fig. 7. The development of overall cd with different tire

At the same time, from Table 1 we can see that the acceleration of the airflow leads to a pressure decline at the bottom of the car, due to tire rotation, reducing the coefficient of lift of the vehicle.

Local Flow Characteristics

Flow Near The Bottom of The Vehicle

From the velocity vector distribution at the bottom of the body in Fig 8, it can be seen that there is no need for baring heat dissipation [9] components at the bottom of the vehicle body such as exhaust pipes which are usually intricately shaped, since the electric vehicle is powered by the battery pack. And it is fitted with a complete cover [10] at the bottom of the model s, making the bottom of the car shape very smooth, it is still stable in high-speed driving conditions.

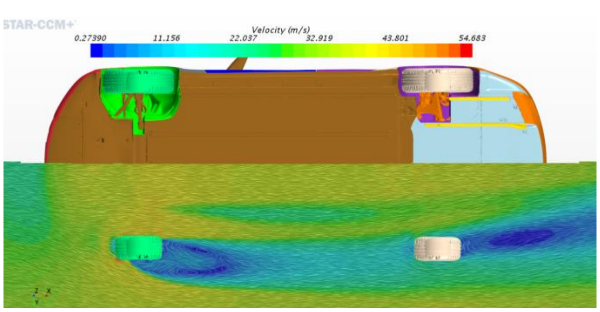

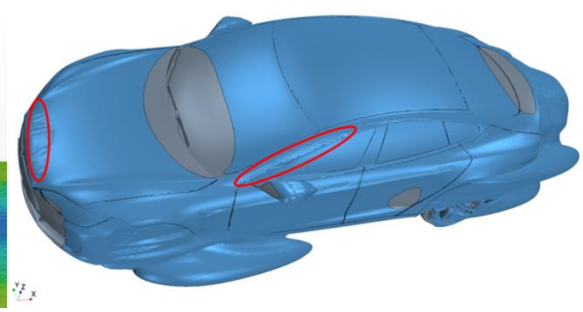

Fig.8. Velocity vector distribution Fig.9. Iso-surface of zero total pressure coefficient

Flow Near The Body Surface

As shown in Fig.9 which show the distribution of iso surface of total pressure coefficient of 0 near the surface of the vehicle body , in addition to the unavoidable flow separation of the rearview mirror and the tires, there are pretty few vortices appearing above the front luggage hood and the A-pillar, while vortices are relatively small near the C-pillar and rear windows where there are usually flow separation [11]. It can be seen that the body shape of the model s is very streamlined, this leads to that the negative pressure area of the vehicle is greatly reduced in high speed driving conditions, which reduces the air drag.

Conclusion

In this paper, we obtained the digital model of Tesla Model S by 3D scanning, and the external aerodynamic characteristics are simulated using STAR-CCM+. Then the coefficient of air drag and coefficient of lift in different working conditions are obtained, and we checked the contribution of each part of the vehicle to the overall coefficient of air drag. The analysis of the flow characteristics and mechanism of air drag reduction is of great significance for reference to the aerodynamic design of passenger cars. At the same time, due to the hasty time, this paper can not analyze the inner flow field, wind noise and so on, hope to continue in the future.

References

[1] Palin R, Johnston V, Johnson S, The Aerodynamic Development of the Tesla Model S - Part 1: Overview. Journal of Shijiazhuang Vocational Technology Institute, 2012

[2] D'Hooge A, Palin R B, Johnson S, The Aerodynamic Development of the Tesla Model S - Part 2: Wheel Design Optimization. 2012.

[3]YingchaoZhang, Numerical Simulation Technology of Automotive Aerodynamics,Beijing, Peking University Press, 2011.

[4] LiminFu, Automotive aerodynamics, Beijing, Mechanical Industry Press, 2006.

[5]Limin, Automotive Design and Aerodynamics,Beijing, Mechanical Industry Press, 2011.

[6]YingchaoZhang, Research on Automobile Wind Tunnel Correction Based on Simulation and Experiment, Changchun, Jilin University, 2010.

[7]LiminFu, Numerical calculation of automobile aerodynamics, Beijing Science and Technology Press, 2011.

[8] Freeman CM, Gaylard AP., Integrating CFD and Experiment: The Jaguar Land Rover Aeroacoustics Process, Mira International Conference on Vehicle Aerodynamics, 2008.

[9] Amodeo J., The Development of CFD as a Primary Design Tool at Jaguar Cars, 5th MIRA International Conference on Vehicle Aerodynamics, 2004.

[10] Gaylard AP., Aerodynamic Development of the New Jaguar XF., Mira International Conference on Vehicle Aerodynamics, 2008.

[11] Samples M., Gaylard AP., and Windsor S., The Aerodynamics Development of the Range Rover Evoque, Mira International Conference on Vehicle Aerodynamics, 2010.